Transactions on Machine Intelligence 1(4) (2018) 204-211

ISSN Online: 2821-1693

Transactions on Machine Intelligence

Journal Homepage: https://tmachineintelligence.ir/index.php/TMI

Evaluation of Grid Performance on Image Quality in Digital Mammography Systems

H. Khodajou Choukami [1,*], B. Vosooghi Vahdat [2], A. Hosseini [3], S. M. Razavi [4]

[1] PhD, Department of Biomedical Engineering, Faculty of Electrical Engineering, Sharif University of Technology, Tehran, Iran
[2] PhD, Department of Biomedical Engineering, Faculty of Electrical Engineering, Sharif University of Technology, Tehran, Iran
[3] PhD, Faculty of Energy Engineering, Sharif University of Technology, Tehran, Iran
[4] MSc, Nik Parto Nuclear Medical Center, Sadeghieh, Tehran, Iran

ARTICLE INFO

Article History:
Received 3 May 2018
Received in revised form 18 July 2018
Accepted 9 December 2018
Available online 11 December 2018

Keywords:
Digital Mammography, Grid, Scattered Radiation, MCNPX Code

ABSTRACT

Mammography is a crucial imaging technique for early breast cancer detection, where image quality plays a vital role in accurate diagnosis. One of the primary factors degrading image quality is scattered radiation, which reduces contrast and obscures fine details. Anti-scatter grids are widely recognized as the most effective tool for mitigating this issue. Initially developed for screen-film mammography, grids have since been integrated into digital mammography systems. However, despite their widespread adoption, their geometric performance in digital systems has not been thoroughly investigated. This study aims to fill this knowledge gap by evaluating the effectiveness of grids in digital mammography. To achieve this, a comprehensive simulation of a mammography system was conducted based on the international standard IEC 60627:2013, utilizing the latest version of the MCNPX 2.7 Monte Carlo code. The signal-to-noise ratio improvement factor (SNRIF) was used as the key metric to assess the impact of grids on image quality. Various grid parameters, including grid ratio, lead strip thickness, and line density, were analyzed to determine their influence on scattered radiation reduction. The simulation results indicate that grids with thinner lead strips, higher grid ratios, and lower line densities significantly enhance image quality in digital mammography. These findings provide valuable insights for optimizing grid design and improving image contrast, ultimately contributing to more accurate breast cancer diagnosis.

1. INTRODUCTION

Breast cancer is the most common type of cancer among women worldwide. When detected early, it is often treatable, making early diagnosis the primary objective of global breast screening programs. Currently, mammography is regarded as the most reliable imaging modality for the detection and screening of breast lesions, particularly breast cancer [1].

Extensive research has been conducted on breast cancer and mammographic imaging. Notably, Rahmani Seryasat and colleagues have presented several studies in this field, including: (A) a novel method for classifying and

* Corresponding Author: Hamidreza.Khodajou@gmail.com
Room 1, 2nd floor, Energy Engineering Department, Sharif University of Technology, Tehran, Iran. P. O. Box: 11155-1639.

http://dx.doi.org/10.47176/TMI.2018.204

segmenting breast cancer tumors, (B) the evaluation of a new computer-aided detection (CAD) system for mass detection in mammography, and (C) the assessment of a novel ensemble learning framework for mass classification in mammographic images [2-4].

In mammography, scattered radiation is the primary factor contributing to image quality degradation [5]. Given the necessity to reduce scattered radiation without increasing the patient dose, extensive efforts have been directed towards optimizing mammographic techniques. Various methods have been proposed to minimize the scattered radiation reaching the image receptor. The linear anti-scatter grid, introduced by Bucky [6] and later refined by Potter [7], has proven to be the most effective device in this regard. Although significant advancements in design and technology have occurred since Bucky's original invention, his foundational work has spurred subsequent innovations. Today, these grids are integral to both digital mammography (DM) and screen-film mammography (SFM) systems.

Researchers have investigated grid performance in both SFM and DM systems. In the context of SFM imaging, experimental studies by Rozen et al. [8] and Monte Carlo simulations by Boone et al. [9] demonstrated that cellular grids exhibit higher contrast improvement factors (CIF) and lower Bucky factors (BF) compared to linear grids. Further studies by Chan et al. [10] indicated that linear grids with lead strip thicknesses of 20-37 micrometers, line densities of 70-100 lines/cm, and grid ratios between 2 and 6 can achieve Bucky factors ranging from 2 to 3.5, resulting in a 40% to 90% contrast enhancement. These results are comparable to those obtained with traditional grids. Subsequent research by Boone et al. [11] revealed that grids with a ratio of 7, gold lamellae thickness of 10 micrometers, and a period of 550 micrometers can produce over 5% higher CIF at the same BF compared to commercial HTC grids from Lorad. However, economic factors may limit the commercial production of these advanced grids [12].

Although studies have been published to evaluate the performance of different grid geometries and models in SFM systems, there is still very limited information available regarding DM systems. Bernhardt et al. [13], Chuck Rabotti [14], and Weltkamp et al. [15] investigated the impact of varying breast thicknesses on image quality in the presence or absence of linear grids. Kana et al. [16] examined this effect in the presence or absence of cellular grids.

In previous studies, some researchers have evaluated the performance of different grid geometries in SFM systems, while others have investigated the impact of varying breast thicknesses on the output images of DM systems in the presence of commercial grid geometries. Therefore, due to the lack of sufficient data on the quantitative evaluation of the performance of different grid geometries in DM systems concerning output image quality, the present study addresses this issue through comprehensive simulation of the mammography system using MCNPX 2.7 code, employing phase space files and a full-energy integrator.

2. MATERIALS AND METHODS

2.1. Definition of Parameters

The quality of digital mammography and film-screen images is primarily degraded by photons scattered from breast tissue. In this context, the use of anti-scatter grids is justified to enhance the quality of both digital and film-screen images. Without accurate quantitative information on the distribution of scattered radiation, it is not possible to evaluate the performance of grids. Therefore, the scatter-to-primary ratio (S/P) has been introduced as a fundamental indicator for estimating the level of contamination present in mammography system images [17, 18].

Geometric parameters are utilized in the design of linear anti-scatter grids. The parameters h, D, and d represent the lead strip thickness, the interspace material thickness, and the grid height, respectively. These are considered independent parameters, while two other important and commonly used parameters, N and r, are derived from these independent parameters, representing the grid ratio and the strip density, respectively [19].

The following equations present the relationships between the grid parameters:

$$r = h/D \quad (1)$$

$$N = 1/(d+D) \quad (2)$$

It is entirely clear that the parameter pairs d and r, as well as h and N, are mutually independent. The evaluation of grid performance in film-screen and digital mammography is conducted using different approaches [16]. For assessing the performance of anti-scatter grids in SFM systems, the Contrast Improvement Factor (CIF) and the Bucky Factor (BF) are utilized. The Scatter Improvement Factor (SIF) is defined as the ratio of the signal-to-noise difference in the presence and absence of the grid. This parameter serves as an appropriate tool for predicting grid performance in digital mammography. As demonstrated by Fetterly and Schueler [21], the SIF parameter can be determined using Equation (6):

$$\mathrm{SIF}=\sqrt{\mathrm{Tp}\times\frac{1+\left(\frac{S}{P}\right)}{1+\left(\frac{S}{P}\right)_{grid}}} \tag{3}$$

Additionally, the SIF can also be expressed in terms of parameters related to the SFM system as follows:

$$SIF=\frac{CIF}{\sqrt{BF}} \tag{4}$$

It is important to note that SIF values less than 1 indicate that the presence of the grid, compared to its absence in the DM system, leads to a reduction in the image signal-to-noise ratio.

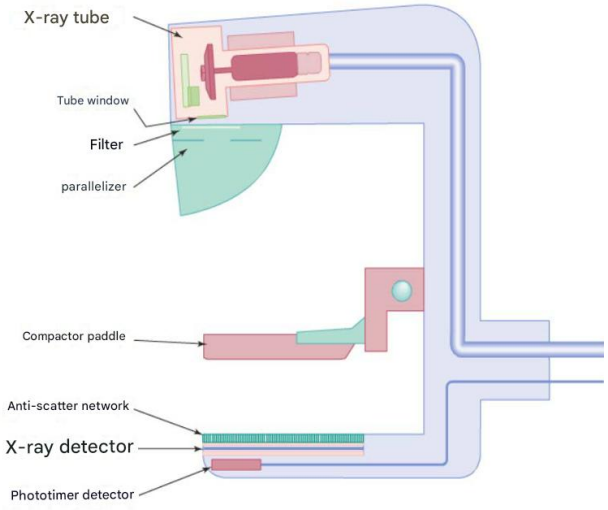

Fig. 1. A Simplified Representation of the Mammography System Geometry and the Grid Placement within the System.

2.2. Modelling and Simulation of the Mammography System Using the MCNPX Monte Carlo Code

In this study, the Monte Carlo N-Particle extended transport code (MCNPX), version 2.7, was used to simulate the mammography system and evaluate the performance of the anti-scatter grid. As shown in Figure 1(a), the mammography system consists of several main components, including the X-ray source, compression paddle, support table, grid, and detector. The various parameters selected for problem definition in the MCNPX code are listed in Table 1. In this study, the X-ray spectrum is similar to that used by Boone et al. [22], with the difference of having a molybdenum (Mo) filter with a thickness of 30 micrometers. After passing through the additional filter, the X-ray beam diverges from the focal spot, resulting in a uniform distribution across the breast surface area [20]. The geometric model of the compressed breast is represented as a semicircular disk containing a mixture of tissues (50% glandular, 50% adipose), surrounded by a 0.5 cm thick layer of adipose tissue. The composition of the breast phantom materials was selected based on the data provided by Hammerstein et al. [23].

In previous studies, such as those by Boone et al. [6, 8] and Kana et al. [16], custom Monte Carlo codes utilized numerical techniques or analytical equations to facilitate photon transport through the grid. However, due to the high capability of the MCNPX Monte Carlo code in particle transport within complex environments, grid simulation in this study has been conducted entirely using the Monte Carlo method. To define the grid, repeated structure cards were employed. Although the use of repeated structures not only reduces the computer memory required for the problem but also decreases the volume of user-defined input, it results in slower execution times [24]. Therefore, to enhance computational speed, the phase space file method was applied [25]. In this approach, the entire problem was divided into two sections. Using a virtual plane, the system was segmented into Region 1, covering components up to the Bucky table, and Region 2, including the Bucky table and the detector system.

In the first run, after particle transport through the components in Region 1, all relevant information and characteristics (type, energy, weight, direction, and position) upon interaction with the virtual plane placed beneath the breast were stored in a phase space file. This file was then utilized in subsequent runs for extensive calculations to evaluate the performance of different grid geometries by linking the transported photons from Region 1 to Region 2 (where the grid is present).

For detector modeling and radiation quantification, the full-energy integrator method proposed by Seelmann-Eggebert et al. [26] was employed. In this model, due to the low energy of X-rays used in mammography, it is assumed that the detector's efficiency in absorbing X-ray photons reaching its surface is 100%, which is logically considered a valid assumption [9, 11].

A simplified model of the mammography system was presented by eliminating components such as the compression paddle and support table. This simplification is consistent with previous works by Boone et al. [9, 11], Dance et al. [20], and Chen et al. [10].

The number of simulated particles in our calculations for generating the phase space file was on the order of 10^9. The relative errors in each simulation were approximately less than 0.5%, with the maximum error reaching 1% under limited conditions.

Table 1. Summary of various parameter selections for mammography system simulation

Distance from focal point to detector surface	0.65 cm
Air gap	5.1cm
Anode-filter combination (thickness)	Molybdenum-Molybdenum(30μm)
Tube voltage	28 kVp
Composition, weight fraction and density of mixed tissue (glandular - ۵۰٪ fat ۵۰٪)	H (0.107), C (0.401), N (0.025), O (0.464), P (0.003), Density= 0.982 g.cm $^{-3}$
Composition, weight fraction, and density of adipose tissue	H (0.112), C (0.619), N (0.017), O (0.251), P (0.001), Density= 0.930 g.cm $^{-3}$
Breast shape	Half cylinder
Breast thickness (T) and radius (R)	T = 5 cm, R = 10 cm
Grid type	Linear
Density and material of the blades	Lead has a density of11.34 g. cm $^{-3}$
Material and fiber density in the interstices of the blades	with a density of 1.32 g. cm $^{-3}$ $(C_6H_{10}O_5)_n$
Blade density(N)	20 – 100 lines per centimeter
Network ratio (r)	17-3
Blade thickness(d)	5 – 30 micrometers
Detector model	Complete energy integrator

3. RESULTS

3.1 Validation

To validate the simulation results, as shown in Figure 2, the scatter-to-primary ratio (SPR) values under different conditions were calculated for various breast thicknesses and tube voltages for breasts with varying diameters (modeled as semi-cylindrical) under identical irradiation conditions, and compared with the reference [18]. The accuracy of all the results obtained from the simulation, in comparison with the reference [18], was confirmed with a deviation of less than 2%.

After confirming and extensively comparing the accuracy of our simulation in Figure 2, data not previously reported in other references were extracted from our calculations and presented in Figures 3(a) and (b). In Figures 3(a) and (b), a representation of the variation of the Scatter Improvement Factor (SIF) as a function of grid geometric specifications is shown. The results demonstrated that, for DM systems, grids with narrower d, lower N, and higher grid ratios exhibited the best performance.

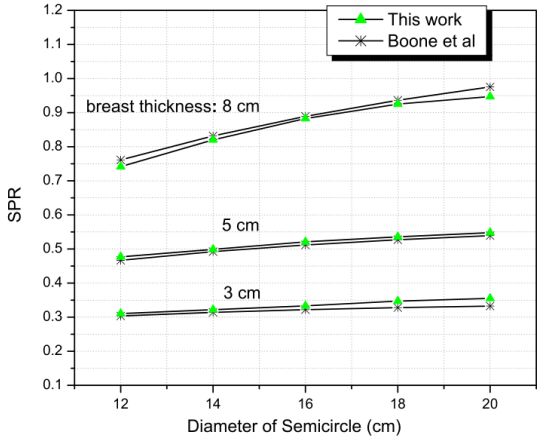

Fig. 2. Comparison of the data obtained from the simulated geometry in the MCNPX 2.7 code with the results available in reference [18].

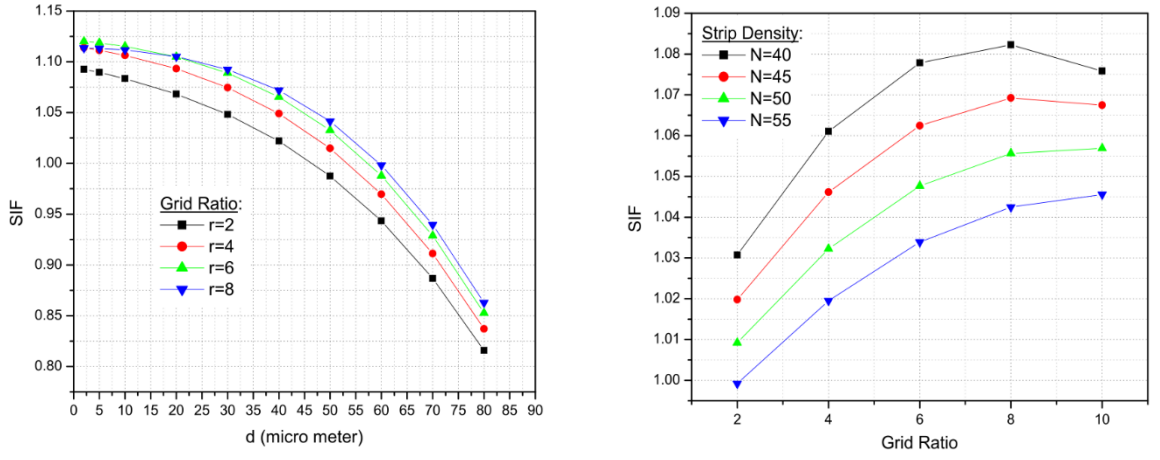

(b) (a)

Figure 3: (a) The Image Signal Improvement Factor in the presence of the grid with a lead strip thickness of 40 μm as a function of *r* at different strip densities.
(b) The Image Signal Improvement Factor as a function of *d* for various grid ratios at a constant strip density of 44 lines per centimeter.

The selection of this grid, providing relatively consistent image quality, results in a minimum relative dose to the patient, which is in exact alignment with the recommendations of the International Atomic Energy Agency (IAEA) [12] regarding the appropriate selection of grids.

4. DISCUSSION AND CONCLUSION

As shown in Figure 2, the validation of the results obtained from the simulation performed using the MCNPX 2.7.0 code, compared to the published data, was confirmed with a deviation of less than 2%. Therefore, this code can be considered an excellent tool for conducting research related to the evaluation of the performance of different grid geometries.

In Figure 3, for the digital mammography system, the highest SIF value corresponds to the grid with the lowest N and smallest d, with the highest grid ratio. Such grids, which produce the highest SIF values, result in the application of the minimum mean glandular dose (MGD) to the breast tissue [16]. To enhance the performance of mammography screening programs, based on the results of this study, the use of separate geometries for digital and film-screen mammography systems is recommended. The geometric features of the grid introduced in this study aim to maximize the signal-to-noise enhancement factor for digital systems.

Transparency Statement

The data supporting this study are available upon reasonable request to the corresponding author, subject to ethical and confidentiality considerations.

Acknowledgments

We would like to express our gratitude to all individuals who contributed to this project.

Declaration of Interest

The authors declare that they have no competing interests.

Funding

This research received no specific grant from any funding agency, commercial, or not-for-profit sectors.

REFERENCES

[1] Ferlay, J., Soerjomataram, I., Dikshit, R., Eser, S., Mathers, C., Rebelo, M., Parkin, D. M., Forman, D., & Bray, F. (2014). Cancer incidence and mortality worldwide: Sources, methods and major patterns in GLOBOCAN 2012. International Journal of Cancer. https://doi.org/10.1002/ijc.29210

[2] Rahmani-Seryasat, O., Haddadnia, J., & Ghayoumi-Zadeh, H. (2015). A new method to classify breast cancer tumors and their fractionation. Ciência e Natura, 37(4), 51–57. https://doi.org/10.5902/2179460X19428

[3] Seryasat, O. R., & Haddadnia, J. (2017). Assessment of a novel computer-aided mass diagnosis system in mammograms. Biomedical Research, 28(7), 3129–3135.

[4] Seryasat, O. R., & Haddadnia, J. (2018). Evaluation of a new ensemble learning framework for mass classification in mammograms. Clinical Breast Cancer, 18(3), e407–e420.

https://doi.org/10.1016/j.clbc.2017.05.009

[5] National Council on Radiation Protection and Measurements. (2004). A guide to mammography and other breast imaging procedures (NCRP Report No. 149).

[6] Bucky, G. (1915). Method of and apparatus for projecting Röntgen images. U.S. Patent No. 1,164,987.

[7] Potter, H. E. (1920). The Bucky diaphragm principle applied to roentgenography. American Journal of Roentgenology, 7, 292–295.

[8] Rezentes, P. S., Almeida, A., & Barnes, G. T. (1999). Mammography grid performance. Radiology, 210(1), 227–232. https://doi.org/10.1148/radiology.210.1.r99dc35227

[9] Boone, J. M., Seibert, J. A., Tang, C. M., & Lane, S. M. (2002). Grid and slot scan scatter reduction in mammography: Comparison by using Monte Carlo techniques. Radiology, 222(2), 519–527. https://doi.org/10.1148/radiol.2222010491

[10] Chan, H. P., Frank, P. H., Doi, K., Iida, N., & Higashida, Y. (1985). Ultra-high-strip-density radiographic grids: A new antiscatter technique for mammography. Radiology, 154(3), 807–815. https://doi.org/10.1148/radiology.154.3.3969487

[11] Boone, J. M., Makarova, O. V., Zyryanov, V. N., Tang, C. M., Mancini, D. C., Moldovan, N., & Divan, R. (2002). Development and Monte Carlo analysis of antiscatter grids for mammography. Technology in Cancer Research & Treatment, 1(6), 441–447. https://doi.org/10.1177/153303460200100604

[12] International Atomic Energy Agency. (2005). Optimization of the radiological protection of patients: Image quality and dose in mammography (coordinated research in Europe) (IAEA-TECDOC-1447).

[13] Bernhardt, P., Mertelmeier, T., & Hoheisel, M. (2006). X-ray spectrum optimization of full-field digital mammography: Simulation and phantom study. Medical Physics, 33(11), 4337–4349. https://doi.org/10.1118/1.2351951

[14] Chakraborty, D. P. (1999). The effect of the antiscatter grid on full-field digital mammography phantom images. Journal of Digital Imaging, 12(1), 12–22. https://doi.org/10.1007/BF03168622

[15] Veldkamp, W. J. H., Thijssen, M. A. O., & Karssemeijer, N. (2003). The value of scatter removal by a grid in full field digital mammography. Medical Physics, 30(8), 1712–1718. https://doi.org/10.1118/1.1584044

[16] Cunha, D. M., Tomal, A., & Poletti, M. E. (2010). Evaluation of scatter-to-primary ratio, grid performance, and normalized average glandular dose in mammography by Monte Carlo simulation including interference and energy broadening effects. Physics in Medicine & Biology, 55(15), 4335–4359. https://doi.org/10.1088/0031-9155/55/15/010

[17] Carlsson, G. A., Carlsson, C. A., Nielsen, B., & Persliden, J. (1986). Generalised use of contrast degradation and contrast improvement factors in diagnostic radiology: Application to vanishing contrast. Physics in Medicine & Biology, 31(7), 737–749. https://doi.org/10.1088/0031-9155/31/7/004

[18] Boone, J. M., Lindfors, K. K., Cooper III, V. N., & Seibert, J. A. (2000). Scatter/primary in mammography: Comprehensive results. Medical Physics, 27(11), 2408–2416. https://doi.org/10.1118/1.1312812

[19] Bonenkamp, J. G., & Boldingh, W. H. (1959). Quality and choice of Potter Bucky grids: III. The choice of a Bucky grid. Acta Radiologica, 52(3), 241–253. https://doi.org/10.1177/028418515905200306

[20] Dance, D. R., & Day, G. J. (1984). The computation of scatter in mammography by Monte Carlo methods.

Physics in Medicine & Biology, 29(3), 237–247. https://doi.org/10.1088/0031-9155/29/3/003

[21] Fetterly, K. A., & Schueler, B. A. (2007). Experimental evaluation of fiber-interspaced antiscatter grids for large patient imaging with digital x-ray systems. Physics in Medicine & Biology, 52(16), 4863–4880. https://doi.org/10.1088/0031-9155/52/16/010

[22] Boone, J. M., Fewell, T. R., & Jennings, R. J. (1997). Molybdenum, rhodium, and tungsten anode spectral models using interpolation polynomials with application to mammography. Medical Physics, 24(11), 1863–1874. https://doi.org/10.1118/1.598100

[23] Hammerstein, G. R., Miller, D. W., White, D. R., Masterson, M. E., Woodard, H. Q., & Laughlin, J. S. (1979). Absorbed radiation dose in mammography. Radiology, 130(2), 485–491. https://doi.org/10.1148/130.2.485

[24] Pelowitz, D. B. (2008). MCNPX User's Manual Version 2.6.0. Los Alamos National Laboratory report LA-CP-07-1473.

[25] Ezzati, A. O., Sohrabpour, M., Mahdavi, S. R., Buzurovic, I., Matthew, & Studenski, M. T. (2014). A comprehensive procedure for characterizing arbitrary azimuthally symmetric photon beams. Physica Medica, 30(2), 191–201. https://doi.org/10.1016/j.ejmp.2013.05.040

[26] Khodajou-Chokami, H., & Sohrabpour, M. (2015). Design of linear anti-scatter grid geometry with optimum performance for screen-film and digital mammography systems. Physics in Medicine & Biology, 60(15), 5753–5765. https://doi.org/10.1088/0031-9155/60/15/5753